 doi:10.20944/preprints202009.0461.v1

Article

A two-step energy management method guided by day-ahead quantile solar forecasts: cross-impacts on four services for smart-buildings

Fausto Calderon-Obaldia [1,2,3,4,5,*], Jordi Badosa [2], Anne Migan-Dubois [3,4] and Vincent Bourdin [5]

[1] Universidad de Costa Rica, San José, Costa Rica; fausto.calderonobaldia@ucr.ac.cr
[2] LMD/IPSL, École Polytechnique, Institut Polytechnique de Paris, ENS, PSL Université, Sorbonne Université, CNRS, Palaiseau France; jordi.badosa@lmd.polytechnique.fr
[3] Universite Pierre et Marie Curie, Paris, France ; anne.migan-dubois@geeps.centralesupelec.fr
[4] GeePs-Laboratoire de génie électrique et électronique de Paris, Gif-sur-Yvette, France; anne.migan-dubois@geeps.centralesupelec.fr
[5] LIMSI-aboratoire d'Informatique pour la Mécanique et les Sciences de l'Ingénieur, Orsay, France; Vincent.Bourdin@limsi.fr
* Correspondence: fausto.calderonobaldia@ucr.ac.cr

Abstract: The research work hereby presented, emerges from the urge to answer the well-known question of how the uncertainty of intermittent renewable sources affects the performance of a microgrid and how could we deal with it. More specifically, we want to evaluate what could be the impact in performance of a microgrid intended to serve a smart-building (powered by photovoltaic panels and with battery energy storage), when the uncertainty of the photovoltaic-production forecasts is considered in the energy management process. For this, several objectives (or services) are targeted based in a two-step (double-objective) energy management framework, that combines optimization-based and rule-based algorithms. The performance is evaluated based on some particular services proposed as performance indicators. Simulations are performed using data of a study-case microgrid (Drahi-Xnovation center, Ecole Polytechnique, France). The use of quantile forecasts (obtained with an analog-ensemble method) is tested as a mean to deal with (i.e. decrease) the uncertainty of the solar PV production. The proposed energy management framework is compared with basic reference strategies and the results show the superior performance of the former in almost all the services and forecasting scenarios proposed. The contrasting nature among some of the target services is one of the main conclusions of this work, as well as the different requirements in terms of forecasts when optimizing for different services and seasons of the year. This fact highlights the usefulness of the quantile forecasting approach, as a tool to deal with the intrinsic uncertainty of PV power production.

Keywords: microgrid; energy-management-system; quantile-forecasts; smart-building

Contents

1. Introduction

When talking about low-power distributed generation with intermittent renewable energy sources (IRES), the concept of microgrids (MGs) comes along as a system that is intended to integrate this type of energy sources into the utility electrical networks. MGs can have different configurations, and according to the classification presented by Zia et al.[1], the system proposed in our work is a DC, centralized, grid-connected, commercial MG.

The energy management (EM) of MGs is still an open research topic, and the variety of approaches is extensive [1][2]. It relates to the strategy used to schedule the resources of the MG (also called distributed energy resources or DERs), that normally respond to specific objectives. At utility scale, this action is called unit commitment (UC).

The techniques commonly used to perform EM vary from case to case, and as mentioned in [1], the supervisory control architecture of an energy management system (EMS) can be divided into two types: centralized and decentralized. At the core of a centralized EMS (such as the one hereby proposed) we find the working objective(s), which is related to a given service that the system is required to deliver and/or optimize. A service provided by a MG could be defined as any action

performed by the system that will improve to some extent the well-being of the users. An example of a typical service provided by a MG would be the cost of the energy, understood as the ability of the MG to offer energy at a competitive cost with respect to the utility grid. In order to achieve the working objective, two main EMS branches can be identified: Optimization-Based (OB-EMS) and Rule-Based (RB-EMS) [3]. The latter can assure attaining the working objective but cannot guarantee an optimal performance, whereas the former can achieve optimal or quasi-optimal performance for a given service. An OB-EMS normally requires a forecast (at least of production and consumption), to issue an optimal action to be followed in the future, which is also called scheduling. The optimization horizon can vary from seconds or minutes (intra-hour) to hours (inter-hour) or days (day-ahead). The optimization objectives can vary a lot, but as pointed out by [4], some of the most common are: carbon emissions, capital and operational costs, energy storage cost and load shedding costs, among others.

The problem of unit commitment under uncertainty related to IRES and MGs in the distribution network has been recognized [5] and efforts are being done in order to deal with it.

At the core of the hereby proposed EMS strategy, we aim at providing a service targeted for the TSO: grid-commitment. It consists in broadcasting to the TSO (one day-ahead) the hourly grid-power-requirements of the MG, and engage (as far as possible) to follow it. However, this scheduled grid profile has been generated in a first stage of the EMS, with a different objective (i.e. energy cost reduction, CO_2 emissions reduction, grid-peak-power reduction). This means that, in a first stage, the MG is "selfish" and looks for its own benefit with the first optimization objective, but once it has generated the grid profile, the second stage of the EMS gives priority to the TSO, as the main beneficiary of the second objective, which is the grid-commitment. This proposal is explained with more details in section 2.3.

A scheduling strategy requires forecasts as an input, and different forecasting methods have been used in the field of energy management for MGs. Some studies directly consider solar generation predictions without considering weather forecasts, while others also receive the information from forecast services [6],[7], or compute it from local power measurements by applying time-series forecasting techniques such as, auto-regressive [8], persistence [9] or ANN [6]. In all these cases, the weather conditions are implicit in the information, but no meteorological variable is directly considered. In other cases, the forecasts of PV power output are directly obtained from weather forecasts, by applying models to transform the meteorological data into output power estimations. These models can be based on real PV panels [10] or theoretical equations of PV generation [11]. Overall, they assume that PV production is fundamentally dependent on irradiance and temperature. Some approaches compute solar irradiance from other parameters such as the clear sky index [12], sky cover [13] or sky clearness [14], rather than forecasting it directly.

The scheduling horizons of the forecasts vary from 72 hours to 15 minutes, depending on the EMS strategy used, however the 24-hour horizon is the most common. The time resolution of those forecasts vary from 3 hours to 15 minutes, being one hour the most common resolution [15].

Regarding the uncertainty, normal distribution is the most frequent option to describe these errors. Some adjustments based on the expectation and the standard deviation are commonly referenced, but they lack of numerical values (e.g. [12]). Other studies assume that forecast errors are well described by a uniform distribution. A thorough summary of the different forecasting techniques used for energy management of MGs can be found in table 1 of the review performed by A. Aguera-Perez et al.[15].

In this work, we propose some basic services for our study-case smart-building (SB), based on the added value they provide to its users and other actors. We tackle the problem of proposing some EMS strategies targeted to provide those services. The services proposed are: grid-commitment, grid-peak-power, energy-cost and carbon-footprint. The definition of these services is explained in detail in section 2.3.

In the domain of MGs, services like grid-commitment or grid-peak-power (introduced in the current work) are not common. This is mostly due to the scale and current penetration of MGs, which is not significant respect to utility grids. But if we imagine a penetration scenario of IRES, that for

Preprints (www.preprints.org) | NOT PEER-REVIEWED | Posted: 20 September 2020 doi:10.20944/preprints202009.0461.v1

2050 could achieve more than 60% according to some studies [16][17] (being distributed generation a non-negligible percentage of it), the capacity to deliver those services could have an important added value, in terms of operational, economic and environmental benefits [18][19]. This is one of the driving motivations of the present work.

However, as the EM strategy usually targets a particular service, a MG can under-perform regarding the non-targeted services, which is one of the main conclusions of this work. Quantile forecasting proved to be an interesting solution not only to customize and optimize performance when targeting a particular service during the EM, but also as a mean to deal with the uncertainty of IRES by providing some degree of certainty regarding the bias of the forecasts. This proved to be beneficial when targeting some services during the EM that are also dependant on different seasonal conditions.

In section 2, a description of the study-case microgrid, the data used and the definition of the services proposed as performance indicators is presented. The Analogs Ensembles method (where the quantile forecasts are obtained) is explained here, as well as the energy management system framework proposed. The reference strategies used to benchmark the performance are also presented in this section. In section 3, the main results and analysis are presented and discussed, while in section 4, the main conclusions of the work are pointed out.

2. Materials and Methods

This study is performed around a real study-case, the MG of the Drahi-Xnovation center, a tertiary-oriented building located on the campus of the École Polytechnique (Palaiseau, France), which is currently being deployed. All the data that has been used in the simulations has been compiled from/for this study-case. The results obtained are also meant to be taken into account for the future implementation of an EMS in this study-case MG. This building is being equipped with PV panels, battery energy storage and some control capabilities that will allow the implementation and test of different EMS strategies, as depicted in Figure 1.

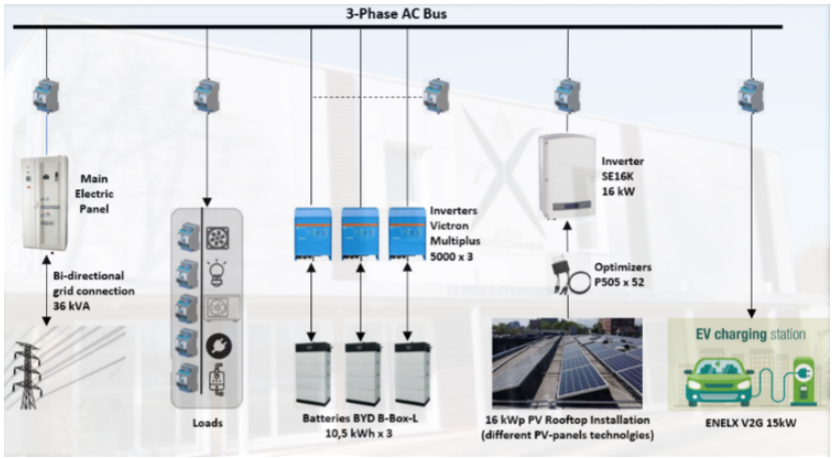

Figure 1. Schematic illustration of the Drahi-X study case microgrid

2.1. The Analogs Ensembles method

Numerical weather prediction (NWP) forecasts from MeteoFrance (ARPEGE) are used in this work as the reference deterministic forecasting method. Forecasts for relative humidity (RH), air temperature measured at 2 meters above ground level (T2) and global solar horizontal irradiance (GHI) are used as the base to generate probabilistic forecasts using the Analogs Ensembles (AnEn) method [20][21]. Clear sky index (CSI) is also required for the AnEn, and it is computed as a ratio between the current GHI (forecasted or measured) and the clear-sky GHI value. Clear-sky GHI estimations are computed using the empirical model proposed by [22].

Preprints (www.preprints.org) | NOT PEER-REVIEWED | Posted: 20 September 2020 doi:10.20944/preprints202009.0461.v1

The workflow principle of the AnEn is shown in Fig. 2, and it is based on the availability of two data-sets with historical data of ground measurements and forecasts. When a new forecast is available for day D+1, it is compared with the forecasts in the database and a certain number of past "similar" forecasts are chosen. The similarity criteria to establish a similarity score between the current forecast (day D+1) and the forecasts in the database is obtained using equation 1.

$$\|F_t, A_{t'}\| = \sum_{i=1}^{N_v} \frac{W_i}{\sigma_{fi}} \sqrt{\sum_{j=t-w}^{t+w} (F_{i,t+j} - A_{i,t'+j})^2} \quad (1)$$

where $\|F_t, A_{t'}\|$ is the error between the forecast for time t and the analog forecast at time t' in the database (similarity score), W_i is the weight of the i^{th} variable, N_v is the number of variables, σ_{f_i} is the standard deviation of the time series of past forecasts of a given variable i, $F_{i,t+j}$ is the forecast of the i^{th} variable at time $t+j$, $A_{i,t'+j}$ is an analog forecast sample of the i^{th} variable at time $t'+j$ and w is the number of hours before and after the target hour that conform the time window, which has a length of $2w+1$.

The corresponding ground measurements to the "similar" forecasts chosen are used to build the ensembles. The AnEn works under the premise that past predictions that are very similar to a given forecast (in terms of meteorological conditions), might present similar errors. This allows to make the pertinent corrections to the current forecast (day D+1), based on the past errors found in the database.

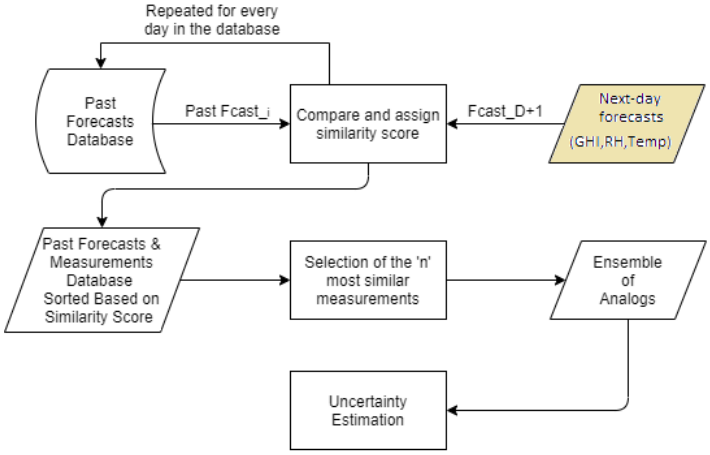

Figure 2. Diagram that sketches the working principle of the AnEn (taken from [20])

From the above-mentioned ensembles, different quantiles are obtained (with probability levels ranging from $AE_{\tau=0.1}$ to $AE_{\tau=0.9}$), which are used as deterministic forecasts. This forecasting approach is called quantile forecasting (QF), and it is used as a novel forecasting method in the domain of MG scheduling. Even when each independent quantile forecast is considered deterministic, the quantile forecasting approach is considered a probabilistic forecasting method, as different quantiles (with different probability levels) can be obtained. The base for this forecasting strategy are the ensembles of analogs (obtained with the above-mentioned AnEn method) from where the quantiles are obtained.

The idea of using this forecasting approach is to decrease the uncertainty of a deterministic forecast by "forcing" the forecasting errors to happen in a known "direction". The hypothesis is that, under certain circumstances (i.e. a particular season and/or service), it could be more beneficial to use over-estimative forecasts, while in other circumstances it might be more beneficial to use under-estimative forecasts. This is a novel way to deal with the intrinsic uncertainty of the PV production without the heavy computational burdens of commonly-used probabilistic optimization methods, such as stochastic programming, which has been used to deal with uncertainty in an EMS of a MG [6], but it is usually demanding in terms of computational resources and time. The QF approach, gives the EMS an interesting capability of adaptation to different conditions as well as target services,

Preprints (www.preprints.org) | NOT PEER-REVIEWED | Posted: 20 September 2020 doi:10.20944/preprints202009.0461.v1

in order to obtain the best performance possible in every situation, with very light computational requirements.

All the data have a time resolution of one hour. The aforementioned forecasts are retrieved for the site of Ecole Polytechnique (Palaiseau, France), while ground measurements for the same site are obtained from the SIRTA atmospheric observatory [23] for the years 2016 to 2018, with the same time resolution. For this work, we considered the forecasts released every 24 hours, at midnight, whose target day is the same day D. The database is split in two periods: the data from the 8^{th} of october 2015 to the 7^{th} october 2017, is used as the historical database required by the AnEn to find the analogs; and the period from the 8^{th} of october 2017 to the 18^{th} october 2018 is used as the test period over which, all the performance indicators are computed.

The expected PV output power of the Drahi-X building is obtained using the GHI forecasts/measurements obtained for the study-case site. With this data, a factor is applied that matches the expected peak-power of the PV-array with the standard solar irradiance conditions (i.e. 1000 W/m^2). This factor does not take into account temperature, shading or tilting effects. Even when this is not a realistic assumption, it was decided to do such simplification as in this work, one of the main objectives is to study the effects of the uncertainty of the solar resource over a MG. Hence, for consistency, GHI is considered as the only stochastic variable and the main source of uncertainty of the PV power output. In this way, the effects of the solar resource uncertainty are isolated, without interference from other sources of uncertainty such as temperature effects, shading and tilting effects or conversion efficiencies of the power converters, that are out of the scope of the present work.

The prices of the electricity are assumed those of EDF (Electricité de France) for the Tempo tariff [24]. The prices vary according to three different types of days: blue, white and red. For each type of day there are two different prices: peak-hour (HP), that goes from 06h00 to 22h00; and non-peak hour (HC), that covers from 22h00 to 06h00. There is also a contracted power monthly fee that has to be paid according to the peak power required from the grid. This contract is annual, meaning that once a given peak power has been contracted, the corresponding monthly fee will be the same throughout the year.

The data of the CO_2 content of the electricity from the utility grid, is taken from the transmission system operator in France, RTE (Réseau de Transport d'Électricité) [25]. They supply real-time and historical data of the energy generation mix and CO_2 footprint of the electricity being produced at every moment of the year. The data has 30 min time steps and were also averaged out to 1-hour time resolution.

It is important to mention that in this work (as implemented by authors like Ferruzzi et al. [26]), the forecasts of electric consumption, prices and carbon footprint of the electricity from utility grid, are always assumed perfect. This is done with the purpose of isolating the effects of the PV power production, and being able to evaluate "independently" its impact upon the EMS strategies. This allows us to study in depth and draw conclusions regarding the effects of its uncertainty in the performance of the SB services, by eliminating possible interference from the uncertainty brought by other stochastic variables. Even when this is not a realistic scenario, by understanding the effects of one stochastic variable (i.e. PV power production), we could comprehend some general mechanisms with which an EMS must deal with, and how it affects the performance of a MG or SB. This knowledge could be applied when integrating other stochastic variables into the game, such as the electrical consumption or the electricity prices.

Benchmark forecasting methods

Persistence (PE) is used as a naive benchmark forecasting method. The forecast is obtained assuming that the hourly PV power profile for day $D+1$ is the same as the one of the previous day D.

Perfect forecasts (PF) are also considered also as benchmark forecasting method, and as its name suggests, it consists on assuming that the forecast of a given variable is actually the real (measured) value of that variable. This is used for PV power output, as the best possible (reference) forecast to compare against the other forecasting methods.

Preprints (www.preprints.org) | NOT PEER-REVIEWED | Posted: 20 September 2020 doi:10.20944/preprints202009.0461.v1

The metrics utilized to measure the forecasting errors are the relative mean-bias error (rMBE), relative mean-absolute error (rMAE) and the relative root-mean-square error (rRMSE), computed as in equations 2, 3 and 4.

$$rMAE = \frac{\frac{1}{H}\sum_{h=1}^{H}\left\|Fcast^h - Meas^h\right\|}{\frac{1}{H}\sum_{h=1}^{H} Meas^h} \tag{2}$$

$$rMBE = \frac{\frac{1}{H}\sum_{h=1}^{H}(Fcast^h - Meas^h)}{\frac{1}{H}\sum_{h=1}^{H} Meas^h} \tag{3}$$

$$rRMSE = \frac{\sqrt{\frac{1}{H}\sum_{h=1}^{H}(Fcast^h - Meas^h)^2}}{\frac{1}{H}\sum_{h=1}^{H} Meas^h} \tag{4}$$

In this study, a generator convention has been used, hence for any DER, positive values of power mean power being delivered by it, while negative values mean power being consumed by the DER.

2.2. *Services and performance indicators*

Four services have been proposed to evaluate the performance of the strategies proposed. A service can be defined as the objective-oriented "actions" that a smart-building can perform (autonomously or semi-autonomously), with the help of a central control system or EMS. The reduction in the cost of the energy consumed by the users of the MG/SB (EC) as well as its carbon footprint ($CO2$), are two of the services chosen, which are well known and commonly used as optimization objectives for EMS strategies, as shown in tables 3,4 and 5 of the comprehensive review performed by ahmad et al. [4]. The other two services we propose, are not common for low-power MGs (they are not even mentioned in the cited review), which are: the day-ahead power commitment with the utility grid or grid-commitment (GC), and the reduction of the grid contracted power or grid-peak-power (GPP).

2.2.1. Service 1: Reduction in energy costs (EC)

The first service is defined as the ability of the SB to provide electricity to its users at a competitive cost with respect to the utility grid. It is always at the top of the list when talking about optimization objectives for EMS in MGs. The associated indicator that allows to quantify this service (its performance indicator), would be the average cost of electricity. This indicator is computed as shown in equation 5, its units are € /kWh and will be hereafter represented by the symbol EC.

$$EC = \frac{1}{E^T_{load}} \cdot \sum_{h=1}^{H}\left(E^h_{grid}\cdot C^h_{grid} + E^h_{batt}\cdot C^h_{batt} + E^h_{pv}\cdot C^h_{pv}\right) \tag{5}$$

where E^T_{load} represents the total energy consumed by the load during the test period, E^h_{grid} is the energy bought from the utility grid, E^h_{batt} is the energy delivered by the battery (battery discharging), E^h_{pv} stands for the PV output energy, while C^h_X represents the cost of the energy of the DER X, at the hour h. The cost of the energy coming from the grid C_{grid} is considered known beforehand for every hour of the test period.

The calculations of the nominal and adjusted costs (accounting for the battery cycling-life reduction and PV curtailment) of the energy coming from the battery and PV panels are presented in Appendix A.1.

2.2.2. Service 2: Reduction in electricity carbon-footprint ($CO2$)

The CO_2 content of the electricity being consumed by the users of the SB is also a common optimization objective searched when performing EM in MGs. Its added value can be understood as

Preprints (www.preprints.org) | NOT PEER-REVIEWED | Posted: 20 September 2020 doi:10.20944/preprints202009.0461.v1

the ability of the SB to provide electricity with less CO_2 content than the electricity coming from the utility grid. The seemingly obvious indicator, used to quantify this service, is the equivalent amount of grams of CO_2 per unit of energy consumed in the MG. This performance indicator can be computed in a similar way as it was presented at equation 5 for the EC indicator. Its units are $gCO2e/kWh$ and will be designated hereafter as $CO2$. The equivalent mathematical expression to compute its value is presented in equation 6.

$$CO2 = \frac{1}{E^T_{load}} \cdot \sum_{h=1}^{H} \left(E^h_{grid} \cdot CO_{2^h_{grid}} + E^h_{batt} \cdot CO_{2^h_{batt}} + E^h_{pv} \cdot CO_{2^h_{pv}} \right) \tag{6}$$

where E^T_{load} represents the total energy consumed by the load during the test period, E^h_{grid} is the energy bought from the utility grid, E^h_{batt} is the energy delivered by the battery (battery discharging) while $CO_{2^h_X}$ represents the CO_2 content, in $gCO2e/kWh$, of the energy coming from the corresponding DER X. It can be either the nominal value (see equation A7 for battery and equation A8 for PV), or the corrected value (see equation A9 for battery and equation A10 for PV). The carbon footprint of the utility-grid energy ($CO_{2^h_{grid}}$) is considered known beforehand [25].

The calculations of the nominal and adjusted values of CO_2 (accounting for the battery cycling-life reduction and PV curtailment) of the energy coming from the battery and PV panels are presented in Appendix A.2.

2.2.3. Service 3: Day-ahead power-commitment with the utility grid (GC)

This service can be thought as the ability of the SB to issue -beforehand-, an hourly-averaged power profile for the upcoming day. The added value of this service lies on the capacity of the MG+EMS of dealing internally with the uncertainty, associated with the renewable production and consumption, by using the energy storage and the curtailment of excess PV energy. The associated performance indicator used to quantify this grid-commitment (GC) service, is computed as the absolute difference between the hourly scheduled and real grid energy profiles. This indicator is normalized with respect to the total-absolute amount of energy scheduled to be exchanged with the grid during the test period. GC is expressed as a percentage, where 100% means a perfect match between scheduled and forecasted energy and 0% represents a deviation equivalent to the scheduled energy to be exchanged with the grid during the test period. This can be more clearly observed in equation 7.

$$GC = 100 \cdot \left\{ 1 - \frac{1}{\sum_{h=1}^{H} \left\| \Delta t \cdot P^{sch_h}_{grid} \right\|} \sum_{h=1}^{H} \Delta t \cdot \left\| P^{real_h}_{grid} - P^{sch_h}_{grid} \right\| \right\} \tag{7}$$

where $P^{real_h}_{grid}$ and $P^{real_h}_{grid}$ are the average-hourly real and scheduled power values exchanged with the grid. Both sums are performed over the total number of hours H of the test period.

2.2.4. Service 4: Reduction of grid contracted-power (GPP)

If the SB-MG surpasses a certain power threshold P^{peak}_{grid}, the utility grid must be ready to deliver that power, even if it is required only few hours of the year. This forces the TSO to have expensive fast-responding generation units idling, that will be required a very small percentage of time. Having these idling plants ready to respond to high power peaks, can increase significantly the cost of the electricity. So the service hereby proposed is meant to decrease this peak power requirements from the MG, an its general added value, if thought in a high penetration scenario, is the reduction of the required installed capacity in the utility grid, which in turns implies a reduction in the cost of the electricity. The performance indicator chosen to quantify this service corresponds to required contracted power according to the EDF-Tempo tariff [24] which allow to contract either 9kW, 12kW, 15kW, 18kW, 30kW or 36kW. This is directly conditioned by the maximum (peak) power in which a given EMS strategy incurs during the test period, hence its designation as the grid-peak-power (GPP).

Preprints (www.preprints.org) | NOT PEER-REVIEWED | Posted: 20 September 2020 doi:10.20944/preprints202009.0461.v1

The lower the GPP, the lower the required contracted power, hence, the lower the annual fee to be paid by the SB users. This is translated in a decrease on the final cost of the electricity consumed by the users of the MG.

2.3. Two-step proposed EMS

Performing energy management consists, in simple words, on actively deciding what resources of a MG are dispatched at every moment and with what level of power, in order to assure the proper functioning of the MG (the balance between production and consumption), and maybe, to favor a secondary objective(s). In order to do that, a system that makes decisions is required, as well as a hardware that allow the execution of those instructions. This process has to be performed at every moment (i.e. in real-time), otherwise the system risks to suffer a blackout. However, sometimes it might be required to plan this real-time resources-dispatching in advance, and for a given window of time (e.g. in day-ahead energy markets). There also services that can only be offered if time-ahead scheduling is performed, as it is the case of the grid-commitment service explained in section 2.2.3. For the above reason, we decided to propose in this work a two-stage EMS strategy, where we separate the day-ahead scheduling from the real-time power balancing. This allows to favor two different objectives (services), one favored by the scheduling module (SCH) and the other favored by the real-time balancing module (BAL), as depicted in figure 3.

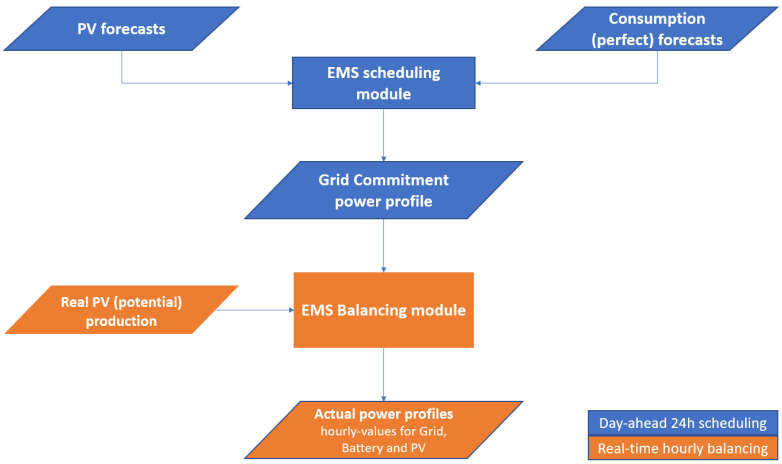

Figure 3. Two-stage EMS proposal

In more detail, in a first stage of the EMS, an optimal scheduling is performed, where three different target objectives (TOs) are possible: energy cost, CO_2 emissions or grid peak-power. During the scheduling stage, only one TO is targeted (i.e. set as optimization objective), depending on the strategy chosen. By definition, all the other services that are not being targeted are called Non-Target Objectives (NTOs). During this first scheduling stage, the grid-commitment service cannot be targeted. A summary of the scheduling strategies along with their objective functions is presented in table 1.

In the second stage of the EMS, once the scheduling module has generated a given grid and battery profiles (i.e. scheduled profiles) -while favoring one of the possible TOs-, it broadcasts the scheduled grid profile to a second module called: the balancing module (BAL). This module targets only one objective: the grid-commitment. This module runs in real-time and therefore is in charge of compensating the forecasting errors of the PV production, by following the rules described in table 1. These rules are explicitly meant to favor the grid-commitment. This means that, the BAL module will modify the scheduled battery profile or perform PV curtailment, in order to preserve the scheduled grid profile untouched, as long as physical constraints allow it (i.e. available capacity on the battery).

This proposal is different to common multi-objective optimization EMS approaches, where the optimal compromise between the different objectives is searched simultaneously during the optimization execution [27][28]. In contrast, our proposal targets a different objective (i.e. service) in

Preprints (www.preprints.org) | NOT PEER-REVIEWED | Posted: 20 September 2020 doi:10.20944/preprints202009.0461.v1

each one of the two stages, (in a "cascade" approach), and using different methods (optimization-based, rule-based). That makes the optimization problem easier to formulate and solve, compared to a multi-objective one. But the main reason why this approach was chosen, is because the grid-commitment, by its nature, cannot be favored in a first EMS stage, as it requires a previously scheduled profile to be followed.

2.3.1. EMS scheduling module

The scheduling module (SCH) of the EMS, performs a day-ahead (D-1) scheduling of the grid average-hourly power requirements for the next day (D). The result of the scheduling is a 24-hour grid power profile. Three different services are proposed as optimization objectives in this stage: the cost of the electricity, the CO_2 content and the grid peak-power. For the first two services the scheduling module make use of a genetic algorithm (GA) to perform the optimization, whereas for the grid peak-power a non-linear programming approach is used. Each method present characteristics that make them more suitable for different optimization objectives. The formulation of the optimization problems for the different -scheduling- target objectives (TOs) is presented in Appendix B.

2.3.2. EMS balancing module

Since the scheduling is performed using day-ahead PV output power forecasts, it is expected to have errors on the forecasted PV power output. The battery is an element that allows to compensate those forecasting errors to some extent, but due to its limited capacity, it could eventually happen that the scheduled grid profiles cannot be followed as expected. In this situation, modifications to the power profiles must be done in order to assure the balance between production and consumption. The balancing module (BAL) is based on rules that are meant to favor the grid commitment, as long as the physical constraints allow it. This means that, any unexpected PV surplus will be stored in the battery, or any lack of PV power required to supply the load, will be supplied by the battery, as long as possible. A flow diagram of the working principle of the BAL module explained above is presented in figure 4.

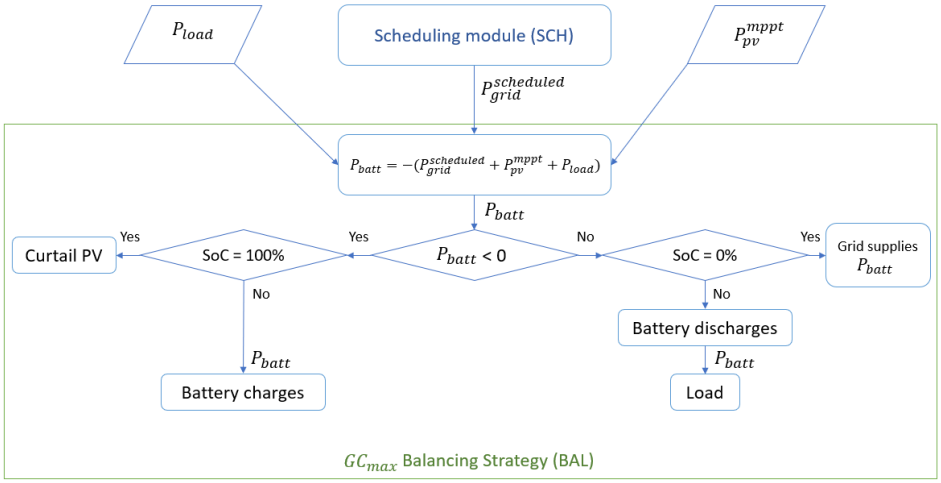

Figure 4. Working principle of the balancing strategy GC_{max}. The output of the scheduling module ($P_{grid}^{scheduled}$), the consumption (P_{load}) and the real PV output (P_{pv}^{mppt}) are the inputs of this module

As it is noted in the rules described above, this module favors the GC service, always assuring the proper balance between production and consumption. In this way, after applying the two-staged EMS, we will have favored two different objectives: GC during the BAL stage and a second objective (i.e. EC, CO2 or GPP) assured during the SCH stage. It must be reminded that during the scheduling stage (SCH) PV curtailment is **not** possible while it **is** possible during the balancing stage (BAL).

Preprints (www.preprints.org) | NOT PEER-REVIEWED | Posted: 20 September 2020 doi:10.20944/preprints202009.0461.v1

A summary of the EMS strategies proposed in this work, including the nomenclature, services favored, working/optimization objectives as well as the possible forecasts to be used, is presented in table 1.

Table 1. Proposed EMS strategies

EMS strategy		Type	Algorithm	Target objective	Objective function / Rules	Possible forecasts
Scheduling (SCH)	EC_{min}	Optimization based	Genetic	Minimize Energy Cost	See equation A11	PF (Perfect Forecast) PE (Persistence) NWP (Numerical Weather Prediction) $AnEn_{\tau=0.1}$ - $AnEn_{\tau=0.9}$ (Analogs-Ensembles quantile forecasts)
	$CO2_{min}$	Optimization based	Genetic	Minimize CO_2 content	See equation A12	
	GPP_{min}	Optimization based	Quadratic Programming	Minimize Grid Peak Power	See equation A13	
Balancing (BAL)	GC_{max}	Rule based	Rules	Maximize Grid commitment	See figure 4	No forecasts used

2.3.3. Reference strategies

The first EMS strategy that is envisaged to be implemented in the Drahi-X smart-building is a basic rule-based balancing-strategy, designated as PVB_{max}. This strategy privileges the use of all the available PV potential (self-consumption) and the battery. Similar variations of this strategy are also commonly used in low-power commercial PV charge controllers, which adds to the interest of using it as a reference strategy. However, the main interest of using this strategy as a benchmark is to observe if the proposed EMS strategies could bring an improvement in performance regarding the services being evaluated. This strategy, even when conceived as a balancing strategy, can also perform scheduling if a forecast of the PV production is given. Therefore, we use this as a reference strategy for both, balancing only (PVB_{max}), and scheduling ($PVB_{max} - NWP$). A flow diagram representing the working principle of the strategy is presented in figure 5.

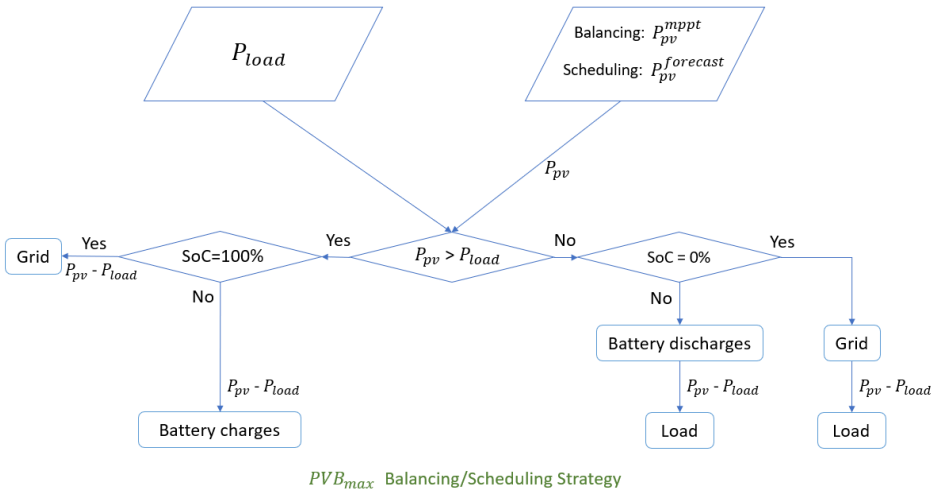

Figure 5. Flow diagram of the reference PVB_{max} strategy. It works as a balancing strategy if real PV-production (P_{pv}^{mppt}) is given, while it performs scheduling if PV forecasts are provided instead ($P_{pv}^{forecast}$)

Preprints (www.preprints.org) | NOT PEER-REVIEWED | Posted: 20 September 2020 doi:10.20944/preprints202009.0461.v1

3. Results

3.1. Performance of the proposed scheduling strategies

Scheduling can be defined as the planning of the use of resources in a MG, for a given window of time in the future. Therefore, derived from this statement, the first advantage of performing scheduling is the ability to offer some services (such as the grid-commitment introduced in this work) that, due to its intrinsic nature, can only be offered if scheduling is performed.

Table 2 summarizes the results in performance of three reference strategies and the three proposed EMS scheduling strategies, regarding the four services under study, denoted by their performance indicators: EC, CO2, GPP and GC. Values in bold represent the best performance obtained for each indicator. In this table, a quantile forecast expressed like: $\text{AnEn}_{\tau=x_1:x_2}$ means that any probability level (i.e. quantile) between x_1 and x_2 produces the same -optimal- performance with the strategy being used.

This cross-comparison against reference strategies is important, as some studies in the field focus only on developing new functionalities or proposing new EMS strategies, without benchmarking against basic reference cases. This is valuable when justifying the necessity or showing the added value of having a MG and/or implementing a novel EMS strategy. The first reference case (maybe the most obvious), is when we assume that there is no MG deployed (**NO MG** in table 2), therefore all the consumption is supplied by the utility grid. The second and third strategies used as reference are the PVB_{max} balancing strategy and the PVB_{max} scheduling strategy, that are presented in detail in section 2.3.2. A summary of the proposed strategies (scheduling and balancing), including the type of algorithm used, the target objective as well as the reference to the objective function equations (when applicable), is presented in table 1.

Table 2. Performance of the optimization-based scheduling strategies with respect to the reference cases. The best-suited forecasting method for each strategy is used

Proposed Strategy strategy	Reference strategy			Performance indicator
	NO MG	$\textbf{PVB}_{\textbf{max}}$	$\textbf{PVB}_{\textbf{max}}-$	
$\textbf{EC}_{min}$-$\text{AnEn}_{\tau=0.5}$	-14.5%	-10.3%	-8.8% ($\text{AnEn}_{\tau=0.1:0.2}$)	**EC** (€/kWh)
$\textbf{CO2}_{min}$-$\text{AnEn}_{\tau=0.3}$	+3.3%	-6.0%	-1.6% ($\text{AnEn}_{\tau=0.1}$)	**CO2** (gCO_2/kWh)
$\textbf{GPP}_{min}$-$\text{AnEn}_{\tau=0.4}$	-36.5%	-9.0%	-36.5% ($\text{AnEn}_{\tau=0.1:0.9}$)	**GPP** (€)

In table 2 we observe that, with the exception of the CO2_{min} strategy, all the proposed scheduling strategies outperform all the reference strategies in the services they target. The exception with the CO_2 content is comprehensible as the embedded CO_2 emissions (due to the manufacturing process) of the battery and PV panels are high, when compared with the carbon footprint of the energy coming from the French national grid.

This results show the importance of developing an EMS strategy that targets the specific service we want to optimize, as it will most likely obtain a better performance than a strategy that is not meant to optimize the same service.

In this particular case, the scheduling method proposed proves to bring an added value to the MG in terms of performance, with respect to the strategy envisaged to be deployed in the Drahi-X building, as long as the proper forecasting method is chosen. This conclusion brings out a question: what does it mean "a proper forecasting method"? What characteristics define it? The answer to this question is addressed in the following section.

3.2. Optimistic and pessimistic forecasts: the versatility of quantile forecasting

At the heart of a scheduling strategy there is always a PV production forecast. An EMS that performs scheduling of DERs, for a given window of time in the future, requires forecasts as inputs. But forecasts are never 100% accurate, then, their intrinsic uncertainty becomes an important subject

Preprints (www.preprints.org) | NOT PEER-REVIEWED | Posted: 20 September 2020 doi:10.20944/preprints202009.0461.v1

to be studied as presumably, this will have an effect on the final performance obtained from a given scheduling strategy.

Recalling the statistical definition of quantile, what the deterministic quantile forecasts say is: if a given quantile τ with probability level x is used as a prediction (i.e. $x_{fcast} = \tau_x$), there will be x% of probability that the bias (i.e. the forecasting error) is positive, being the bias computed as the difference between the forecast value and the observation (i.e. $B = x_{fcast} - x_{obs}$). This is an interesting characteristic of the quantile forecasting method as it allows the decomposition of the bias or forecasting error E_{fcast} in two components, namely: the -absolute- magnitude and a the sense or direction. Quantile forecasting allows us to choose (to some extent) between the absolute magnitude and the sense or direction of the forecasting error, which can be beneficial in an application where having a bias in a given direction is more beneficial than having it in the other direction (or not having it at all).

The results are obtained for the entire test period and are summarized in table 3. In this table, the GC indicator is also included, as grid-commitment is a common service to all the scheduling strategies (EC_{min}, $CO2_{min}$ and GPP_{min}), assured by the balancing module (BAL). We show here the results of using a very pessimistic forecast ($AnEn_{\tau=0.1}$; rMBE=-0.354, rMAE=0.384), a very optimistic forecast ($AnEn_{\tau=0.9}$; rMBE=0.316, rMAE=0.329), a quasi-unbiased forecast (PE; rMBE=-0.001, rMAE=0.372), a low-bias high-accuracy forecast (NWP; rMBE=-0.002, rMAE=0.219) and a perfect forecast (PF; rMBE=rMAE=0).

Table 3. Impact in performance of different types of forecasts

Scheduling Strategy	Performance Indicator	**$AnEn_{\tau=0.1}$** (Pesimistic Forecast)	**$AnEn_{\tau=0.9}$** (Optimistic Forecast)	**PE** (Unbiased Forecast[1])	**NWP** (Reference Forecast)	**PF** (Most Accurate Forecast)
EC_{min}	EC (€/kWh)	0.297	0.217	0.176	0.169	**0.154**
	GC (%)	99.9	92.1	96.2	99.1	100
$CO2_{min}$	CO2 (gCO_2/kWh)	73	89	65	64	**63**
	GC (%)	99.9	88.1	94.3	98.5	100
GPP_{min}	GPP (kW)	15	18	15	18	**15**
	GC (%)	99.7	90.8	95.3	99.1	100

As states in table 3, the best results (bold values) for all indicators are obtained with the most accurate forecast PF, with a 100% of GC for the three scheduling strategies as well as the smallest values for EC, CO2 and GPP. This is consequent as the optimal strategies found during scheduling are being strictly followed when a perfect forecast is used (the most accurate forecast possible), hence the optimal performance is achieved. However, this scenario is unrealistic as having a perfect PV-power forecast is most likely unachievable.

Regarding the EC_{min} strategy, we observe some correlation with the bias of the forecasting error, as EC presents its highest (worst) value with the most pessimistic forecast ($AnEn_{\tau=0.1}$), followed by the most optimistic forecast ($AnEn_{\tau=0.9}$) and the low-bias high-absolute-error forecast (PE). It seems that this service requires low-bias and low-absolute-error forecasts to yield its best performance, as it is the case when using the NWP and PF. The difference between the best and the worst strategies (EC_{min}-PF and EC_{min}-$AnEn_{\tau=0.1}$ respectively) are as high as 92.8%, which represent an increase in the price of the electricity of 0.14 € /kWh. However, it must be remarked that the smallest cost obtained (using EC_{min}-PF) is about 0.154 € /kWh, which is competitive with the tempo tariff only in the peak hours of the white and red days, where the electricity price is higher than this value. This remarks the importance of optimally deciding when to store/use energy from the battery, and when is better to buy the energy directly from the utility grid, in order to optimize this service.

Regarding the CO2 indicator, the highest value is obtained with the most optimistic forecast ($AnEn_{\tau=0.9}$) forecast, which is 41.2% higher than the reference PF case, followed by the $AnEn_{\tau=0.1}$

[1] Aside from the perfect forecast (PF)

 doi:10.20944/preprints202009.0461.v1

approach (+15.9%), the persistence approach (+3.2%) closing with the NWP forecasting method that presents only an increase of +1.6% with respect to the reference PF approach. There is a clear difference here between the results of the quantile forecasts ($AnEn_{\tau=0.1}$,$AnEn_{\tau=0.9}$) and the other two forecasting methods (PE, NWP), which suggests that this service is favored by low-bias forecasts.

The carbon footprint when using the $CO2_{min}$-PF strategy, is 63 gCO_2/kWh which is higher than the mean and the mode of the carbon footprint associated to the electricity coming from the utility grid. This fact helps to explain the results obtained in table 2, that show that the average CO_2 content is higher when a MG is deployed, due to the high embedded CO_2 emissions of the battery and the solar panels.

Regarding the GPP_{min} strategy, the behavior is a little bit different. In this case, the smallest contracted power (i.e. the best performance) is obtained with the most pessimistic ($AnEn_{\tau=0.1}$), most unbiased (PE) and most accurate (PF) forecasts, at the same time. From this fact, it could be concluded that optimistic forecasts such as $AnEn_{\tau=0.9}$, are not favorable for the grid-peak-power service. This might result from the fact that, under-estimative (or unbiased) forecasts, are more likely to have errors that result in battery getting fully charged, hence, promoting the PV curtailment. When this happens, the scheduled -smooth- grid profile produced by the GPP_{min} strategy remains less modified. A similar situation happens when the PF is used, as it does not produce changes to the scheduled grid profile. This is not the case when using the NWP forecasts, as it has a more over-estimative tendency compared to PE or $AnEn_{\tau=0.1}$. For this indicator, the use of the $AnEn_{\tau=0.9}$ and NWP forecasts, leads to an increase of 9.8% in the annual fee.

A similar phenomena occurs with the grid-commitment for the three scheduling strategies, where the $AnEn_{\tau=0.1}$ forecast, being the most pessimistic, presents the best results. This seems to confirm the fact that under-estimative (i.e pessimistic) PV power forecasts, favor the grid-commitment service. The latter throws an interesting conclusion regarding the effect of forecasts accuracy: highly optimistic or pessimistic forecasts (such as $AnEn_{\tau=0.9}$ or $AnEn_{\tau=0.1}$), do affect negatively the performance in some services like EC or CO_2 content, that seem to be rather favored by low-bias forecasts (e.g. PE or NWP). On the other hand, a service like grid-commitment seems to be favored by pessimistic forecasts, while the grid contracted power, while not presenting a clearly defined behaviour, seems to "prefer avoiding" optimistic forecasts.

With the previous results in mind, an EMS seems to be able to favor some services by using different forecasting approaches with errors ranging from under-estimative to over-estimative. This suggests that it does not exist an unique proper forecasting method as such, as it is dependent on the service being targeted. Therefore, if the most suitable forecasts are used for each service, how well can the EMS perform? To what extent can we improve performance in the services proposed? We try to find the answer to this question in the next section

The results shown so far, might suggest that there might be services that might benefit from over or under estimative forecasts, then we try to discover in the following section, what is the optimal quantile forecast that must be used in order to optimize the different services under analysis.

3.3. Optimizing the services: finding the best-suited quantile forecasts

It must be recalled that an optimization-based EMS, such as the ones proposed in this work, require deterministic forecasts of PV production. Therefore, quantile forecasts are a way to provide the EMS with a deterministic forecast that has intrinsic probabilistic information embedded. More specifically, the most valuable information that we can extract from a quantile forecast is the probability of the error being either over or under estimative. By knowing this information in advanced we can deliberately use the forecasts that are best suited for the service being targeted during the scheduling.

The results presented in figure 6 include the PV costs, reduction in the expected TOE of the PV array due to curtailment, as well as the correction in battery cycling life. In other words, the electricity cost and CO_2 content for the battery and PV energy is affected by the profile of use, following equations A3, A6, A9 and A10.

Preprints (www.preprints.org) | NOT PEER-REVIEWED | Posted: 20 September 2020 doi:10.20944/preprints202009.0461.v1

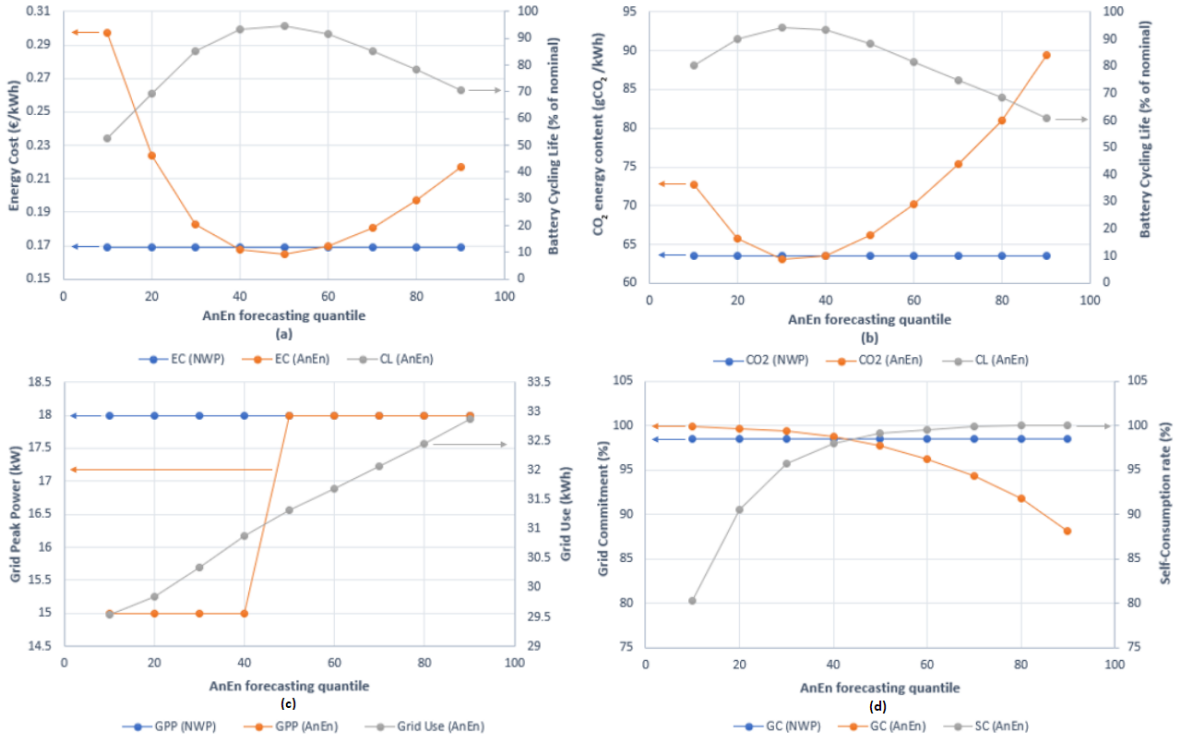

Figure 6. Impact of probabilistic forecasts in: (a) the energy cost (EC) using the EC_{min} scheduling strategy; (b) the carbon footprint (CO2) using the $CO2_{min}$ scheduling strategy; (c) the grid peak-power (GPP) using the GPP_{min} strategy and (d) the grid-commitment (GC) and self-consumption rate (SC) using the $CO2_{min}$ scheduling strategy. Results include correction for projected battery cycling life reduction (relative to nominal) and PV curtailment

The results shown in figure 6(a) are obtained with the EC_{min} scheduling strategy, while the ones of figure 6(b) are obtained with the $CO2_{min}$ scheduling strategy. In both plots, the battery life is presented as a gray curve that represents the battery cycling life as a percentage of the nominal cycling life (i.e. the maximum possible cycling life).

It seems that in both cases, the reduction in battery life, plays a major role in the behaviour of both EC and CO2 indicators, as they find its minimum value where the battery life is maximum. In both cases, the quantile forecasts permit to obtain a better performance (however marginal) than NWP, being EC and CO2 2.4% and 0.7% less than the values obtained using NWP, respectively. It is important to remark than the best performance for the EC is obtained using the $AnEn_{\tau=0.5}$ forecast, while the lowest carbon footprint is found using the $AnEn_{\tau=0.3}$ quantile forecast. This is important because it remarks the fact that not always the most accurate forecast (i.e. the one presenting the smallest rMAE or rRMSE) yields the best performance in every service.

Regarding the minimization of the contracted power observed in figure 6(c), quantiles forecasts below $AnEn_{\tau=0.4}$, allow a reduction of 16.6% with respect to the NWP forecasts. Above $AnEn_{\tau=0.5}$, the performance is the same for both, quantile forecasts and NWP, that allow a contracted power of 18kW, according to the tempo tariff. This fact can be explained as for higher quantiles there is over-estimation of the PV production, which would lead to a situation where the system will empty the battery and will make use of the grid in order to compensate for the over-estimations of PV production.

If we look at the grid-commitment in figure 6(d) (GC-orange curve), it presents a pseudo-parabolic decrease with the increase of the quantile. In contrast, we observe that the self-consumption (SC-gray curve) increases following also a pseudo-parabolic pattern. This can be simply explained as follows: over-estimative forecasts (i.e. high quantiles) provoke errors that have to be counteracted by the grid, as it foresees more PV production than the actual. Therefore, all the PV power available is used

Preprints (www.preprints.org) | NOT PEER-REVIEWED | Posted: 20 September 2020 doi:10.20944/preprints202009.0461.v1

(SC=100%), but the grid deviates from its scheduled profile to compensate the errors (which implies lower GC). On the other hand, for under-estimative forecasts (i.e. low quantile forecasts), there will be excess of PV power that is counteracted by means of PV power curtailment (i.e. lower SC), when the battery gets full. In the latter case, the MG is able to follow closely the scheduled grid power profile, yielding the highest values of GC. The highest performance (GC = 100%) is obtained with the $\text{AnEn}_{\tau=0.1}$ quantile forecast (that is, at the same time, the least accurate), and it outperforms NWP by 1.5%.

In this section, we realized the advantage of the quantile forecasts, that give us the flexibility to "choose", to some extent, the desired direction of the bias (or forecasting error), in order to favor a given service. Using these results, we managed to improve the performance of the services (independently) to a certain extent, and we found the best combinations of scheduling-strategy+forecasting-method for each service (graphically seen in figure 6). However, given that the best combination of scheduling-strategy + forecasting-method is different for each service, when we chose to optimize one service, what is the impact over the other services? Can we find a strategy that produces a good performance for all services? This question is tackled in the following section.

3.4. How optimizing for one service affect the performance on the other services

This section explore how performing optimal scheduling targeting a particular service, affect the performance of the non-targeted services. If so, it would be of interest to know in which way and to what extend those other services are affected. In order to answer this question, the best combination of scheduling strategy+forecast, for each one of the services, is run for the test period. As usual, the output of the scheduling module passes through the BAL module before outputing the final power profiles. In this way, the performance of each scheduling strategy regarding its target and not-target services can be cross-compared, to see the impact among the different strategies.

All these results are summarized in table 4, where the numbers in bold represent the best values obtained for each service, and the positive/negative bias represents a relative increase/decrease of the corresponding performance indicator with respect to the best performance obtained for that service. In this table, the percentage with respect to the best result of the GPP indicator, represents the percentage-difference in terms of the annual fee that must be paid depending on the contracted power required, as it was considered more meaningful for the purposes of the comparison of this indicator.

There are two main results to take away from this table, being the first one the fact that the best performance in each service, is obtained when using the scheduling-strategy-plus-forecast that targets that service. This validates the usefulness of the proposed scheduling strategies, as they allow to produce improvements in performance in every service studied. The second interesting fact, and related to the previous one, is that a scheduling strategy always under-performs for those services it does not target. For instance, in the case of EC, the best performance (0.165 € /kWh) is obtained with the EC_{min}-$\text{AnEn}_{\tau=0.5}$ scheduling strategy. Its performance in the other services is always sub-optimal. Regarding CO_2, the best performance is obtained with the CO2_{min}-$\text{AnEn}_{\tau=0.3}$ strategy (63 gCO_2/kWh), and the GPP_{min}-$\text{AnEn}_{\tau=0.4}$ yields the best performance in GPP (15 kW). Regarding the grid-commitment, it is not favored by any scheduling module, but by the balancing module, that is present for all the scheduling strategies. However, based on the results obtained for the test period, it was found that the EC_{min}-$\text{AnEn}_{\tau=0.1}$ combination, produced the best annual performance for this service, among the different strategies.

Another important fact that comes back again in this results is that, in order to obtain the best performance in each service, different (quantile) forecasts must be used (that are not always the ones presenting the smallest absolute errors rMAE, rRMSE). That highlights the importance of the versatility provided by use of the quantile forecasts obtained with the AnEn method, that outperform results obtained with the reference NWP forecasts. Now, it is reasonable to wonder if it is possible to find a strategy that produces a good compromise, in terms of performance, among all services. It is true that, sometimes, the price to pay in order to achieve the best performance in one -target- service is

Preprints (www.preprints.org) | NOT PEER-REVIEWED | Posted: 20 September 2020 doi:10.20944/preprints202009.0461.v1

big (regarding the remaining services), and the superiority in the target service might be marginal, with respect to the other strategies. For instance, if we take the EC_{min}-$AnEn_{\tau=0.1}$ strategy, it yields the best performance for the grid-commitment service, with a value of 99.9%. However, the advantage in performance of this indicator with respect to the other strategies is not huge, as the worst performer in this indicator is the EC_{min}-$AnEn_{\tau=0.5}$ strategy, which under-performs by only 1.2%. At the same time, the "price" in terms of performance of the not-targeted services that we have to pay if we want to obtain the best GC performance, is very big (with values up to +66.5% in carbon footprint, +80% regarding EC or -57.4% in GPP). At the view of the above, it might not be worth it to use the EC_{min}-$AnEn_{\tau=0.1}$ strategy, and rather it would be more beneficial to choose another one that produces a better compromise among all services. If we observe the strategy that presents the smallest under-performance values of all, is the GPP_{min}-$AnEn_{\tau=0.4}$. So we could say that this strategy presents the best compromise for all the services, followed by the EC_{min}-$AnEn_{\tau=0.5}$ strategy.

Table 4. Impact of targeting one service during the scheduling over the non-targeted services. Quantile forecasts used

EMS	$\mathbf{EC}_{min} - AnEn_{\tau=0.5}$		$\mathbf{CO2}_{min} - AnEn_{\tau=0.3}$		$\mathbf{GPP}_{min} - AnEn_{\tau=0.4}$		$\mathbf{EC}_{min} - AnEn_{\tau=0.1}$	
Intended to:	Minimize EC favor GC		Minimize CO_2 favor GC		Minimize GPP favor GC		Minimize EC favor GC	
Performance indicator		% respect to the best:		% respect to the best:		% respect to the best:		% respect to the best:
EC (€/kWh)	**0.165**	0.0	0.173	+4.8	0.177	+7.3	0.297	+80.0
CO2 (gCO_2/kWh)	65	+3.3	**63**	0.0	64	+1.9	105	+66.5
GPP (kW)	30	+57.4	30	+57.4	**15**	0.0	30	+57.4
GC (%)	98.7	-1.2	99.4	-0.5	99.3	-0.6	**99.9**	0.0

From this section we conclude that targeting one service (with its best scheduling-strategy + forecasting-method) affects negatively the performance on the other services (i.e. the best performance of each service is only achieved when the best combination of scheduling-strategy + forecasting-method for that particular service is used). However, a good compromise can be found with some combinations that yield satisfactory performance for all services. At the view of the above we wonder: can these results be affected by different seasonal conditions? How can these best combinations of "scheduling-strategy+forecasting-method" be adapted for each season? Could we further improve performance by applying seasonal EMS strategies rather than annual strategies? The answers to these queries are tackled in the following section.

3.5. Seasonal performance optimization and analyses

As every building is exposed to different conditions that have a seasonal behaviour (i.e. different degrees of accuracy of the PV forecasts, different PV production and consumption patterns, different prices of electricity and CO_2 content), the last question that arises regarding this analysis is: how much these seasonal effects can affect either positively or negatively the performance of a SB?

In order to answer this question, we take the best EMS strategy (i.e. best combination of scheduling strategy and quantile forecast) based on their performance for each service and for each season of the year. The summary of these strategies is presented in table 5. In this table, when a quantile forecast has two quantiles (e.g. $AnEn_{\tau=10:90}$), it means that any quantile from $AnEn_{\tau=0.1}$ to $AnEn_{\tau=0.9}$ yields the same (optimal) results for that strategy. It is already very interesting to note how, for a given scheduling strategy, the forecasts that produce the best results can be so different between seasons. For instance, if we use the $CO2_{min}$ scheduling strategy, we require the $AnEn_{\tau=0.1}$ forecast in autumn to obtain the best results, whereas in summer or spring, is the $AnEn_{\tau=0.4}$ forecast the one that yields the best performance. In contrast, when using the GPP_{min} strategy, any quantile forecast will produce the optimal performance in autumn, while is the $AnEn_{\tau=0.2}$ only in winter, that produces the best results. The versatility of using quantile forecasts for energy management is again highlighted here, as it permits to customize an EMS according to a particular service and season of the year, to obtain

Preprints (www.preprints.org) | NOT PEER-REVIEWED | Posted: 20 September 2020 doi:10.20944/preprints202009.0461.v1

optimal performance. The strategies described in table 5 are run for each season, and the results are summarized in table 6. The values in parenthesis represent the percentage difference with respect to case when the same scheduling strategies are run using the -reference- NWP forecasts.

We observe in these results that, most of the scheduling strategies that use quantile forecasts, achieved a better performance than the same scheduling strategies using NWP forecasts. The exception is the GPP during spring, summer and autumn, where there is no improvement, and the carbon footprint in summer that presented a marginal increase when using quantile forecasts. Even when some of the improvements are marginal, there are some others that are significant, such as the carbon footprint in autumn, that decreased 24.1% or the GPP in winter that decreased 16.7% when using quantile forecasts instead of NWP. This supports the added value of using quantile forecasts in energy management to obtain better performance by customizing the EMS strategy to different operating conditions and requirements.

Regarding the seasonality differences, we see clearly that, with the exception of grid-commitment (that achieved a 100% in all seasons), for the rest of services (i.e. EC, CO2 and GPP), the performance is always better in summer and spring and worst during winter and autumn. It must be recalled that several factors play a role in the differences in performance for the different services. Common to all of them, there is the annual variations in the consumption patterns. There is also the annual variability in PV output power (i.e. PV power availability), where the intensity in the PV power available as well as the longer duration of the night during winter months, is a factor that clearly impacts the performance of a system powered by photovoltaic panels.

As mentioned previously, the accuracy of the forecasts also changes throughout the year. Besides the above mentioned aspects (common to all scheduling strategies), EC_{min} and $CO2_{min}$ are affected by the variations of the prices and CO_2 content of the electricity coming from the grid. The sum of the effects of all these aspects, condition the response of the different scheduling strategies that try to find a way to achieve their goals under these constraints.

Table 5. Best combinations of scheduling strategy and forecasting method for the different seasons and services

Performance indicator	Best Winter EMS	Best Spring EMS	Best Summer EMS	Best Autumn EMS
EC (€/kWh)	$EC_{min} - AnEn_{\tau=0.6}$	$EC_{min} - AnEn_{\tau=0.5}$	$EC_{min} - AnEn_{\tau=40:50}$	$EC_{min} - AnEn_{\tau=50:60}$
CO2 (gCO_2/kWh)	$CO2_{min} - AnEn_{\tau=0.3}$	$CO2_{min} - AnEn_{\tau=0.4}$	$CO2_{min} - AnEn_{\tau=0.4}$	$CO2_{min} - AnEn_{\tau=0.1}$
GPP (kW)	$GPP_{min} - AnEn_{\tau=0.2}$	$GPP_{min} - AnEn_{\tau=0.2:0.3}$	$GPP_{min} - AnEn_{\tau=0.1:0.8}$	$GPP_{min} - AnEn_{\tau=0.1:0.9}$
GC (%)	$EC_{min} - AnEn_{\tau=0.2}$	$EC_{min} - AnEn_{\tau=0.1:0.2}$	$EC_{min} - AnEn_{\tau=0.1}$	$EC_{min} - AnEn_{\tau=0.1}$

Table 6. Seasonal performance using the strategies of table 5. Values in parenthesis respresent performance with respect to the performance obtained when using NWP

Performance indicator	Winter	Spring	Summer	Autumn
EC (€/kWh)	0.236 (-1.7%)	0.114 (-2.6%)	0.091 (-5.2%)	0.173 (-2.2%)
CO2 (gCO_2/kWh)	58 (-2.1%)	53 (-0.6%)	56 (+1.1%)	89 (-24.1%)
GPP (kW)	15 (-16.7%)	12 (0%)	9 (0%)	15 (0%)
GC (%)	100 (+0.4%)	100 (+1.8%)	100 (+1.6%)	100 (+0.1%)

A third question that arises after the results presented so far in this section, is if adopting a seasonal EMS strategy (i.e. using the strategies of table 5 during the corresponding season) produce better results, by the end of the test period, than using a unique EMS strategy for each service (i.e. EMS strategies of table 4) during the entire test period. The values in parenthesis of the seasonal strategies represent their percentage performance with respect to the case when the best annual-strategy for each service is used.

The results are summarized in table 7, where we can observe that for the grid-commitment, the seasonal strategy presents only a marginal improvement of 0.1% over the annual strategy. Similarly, for the grid-peak-power there is no difference between both approaches. On the other hand, we have a

Preprints (www.preprints.org) | NOT PEER-REVIEWED | Posted: 20 September 2020 doi:10.20944/preprints202009.0461.v1

marginal decrease of 0.5% in the CO_2 content for the seasonal strategy respect to the annual strategy, whereas the energy-cost experience a more significant reduction of 9.1% if the seasonal strategy is used. We can conclude then that the seasonal strategy presents an overall better performance with respect to the annual strategy. At the view of the results presented in table 5, where it is clearly stated that for the different seasons of the year, different forecasting methods should be used in order to obtain the optimal performance. Therefore, an annual strategy, that makes use of a single forecast throughout the test period, is expected to under-perform a seasonal strategy.

Table 7. Performance obtained using a seasonal and an annual energy management strategy

Performance indicator	EMS strategy	
	Seasonal	Annual
EC (€/kWh)	0.150 (-9.1%)	0.165
CO2 (gCO_2/kWh)	62.8 (-0.5%)	63.1
GPP (kW)	15 (0%)	15
GC (%)	100 (+0.1%)	99.9

We can then conclude that seasonal effects such as: prices of electricity, CO2 content, accuracy of forecasts, consumption and production patterns, do affect the performance in the services under study. There are seasons that present conditions that allow better performance (summer, spring) than others (winter, autumn). Best seasonal strategies are different than annual strategies and we proved that using seasonal strategies yield better performance than using annual strategies in some services such as the energy-cost, while for other services it seems to be indifferent (e.g. GPP).

4. Conclusions

A new framework methodology for energy management in buildings that are equipped with a photovoltaic (PV) plant and a battery storage system has been presented. For this, we have considered four possible services for smart buildings consisting in improving the energy cost (EC), the CO2 cost, the grid peak power (GPP) and a grid commitment (GC). The system targets those services using a two-step energy management framework consisting of: a scheduling module and a balancing module. The scheduling module takes PV quantile forecasts which are used to decide the hour-by-hour energy exchanges with the grid for the following day, while favoring one of the services (i.e. EC, CO2 or GPP). Results shows that an EMS with optimization-based scheduling strategies, as the ones hereby proposed, is able to outperform the different reference strategies in every service, with improvements up to 50% in some cases, with the exception of the carbon footprint, where having no microgrid (MG) produces, in average, 4.9% less carbon emissions. From this result, it is important to remark that, taking into account the embedded CO_2 emissions of the battery and PV panels, as well as the electricity mix of the country, play an important role in defining if the implementation of a MG, or a given energy management strategy, can provide reductions in CO_2 emissions or not.

More accurate forecasts (e.g. NWP compared to eccentric quantiles from the analog ensemble method) are seen to result in a better performance, particularly for EC and CO2 indicators. However, for some services, in particular the grid-commitment and grid-peak-power, and for some optimisation periods, this is not the case. This is particularly seen for the seasonal analysis, where in order to obtain optimal performance in the different seasons of the year, different quantile forecasts are to be used. It seems that for some services, the fact of knowing the sense of the forecasting error (i.e. if it is an under or over-estimative forecast) is more beneficial than having a very accurate forecast (i.e. with very low rMAE or rRMSE). In this way, quantile forecasts allow to customize the EMS strategies to different services and weather conditions. The EMS tends to counteract the errors of pessimistic forecasts via PV curtailment, while it compensates the errors of optimistic forecasts mostly using the grid. Hence, if a service such as GC is the optimization objective, pessimistic forecasts (i.e. quantiles less than $AnEn_{\tau=0.5}$) produce the best results. In an annual-based analysis, quantile forecasts permit to obtain better performance in EC, CO2 and GC, in comparison with the deterministic NWP forecasts. However,

the improvement is mostly marginal. At the same time, in a seasonal-based analysis, the advantages of using quantile forecasts can be more significant, achieving improvements in performance of 16.7% for GPP during winter or 24.1% for CO_2 emissions during autumn, with respect to the base-case with NWP forecasts. We also realized the importance of including the cost and embedded carbon content of the energy delivered by the battery and PV panels in the calculations, as well as the significance of correcting those values based on the battery-cycling-life reduction and PV power curtailment. Those aspects showed to have an important impact not only in the magnitude of the resulting values of performance, but also in their behaviour.

Results confirm that the best service indicator is found when the scheduling optimization is oriented for that service. This implies that when the scheduling strategy optimizes for one service (i.e. its target service), the system will under-perform in the other services (i.e. the non-targeted services).

In the search of a strategy that presents a good compromise in performance among all services, we observe that targeting the grid-commitment is the most expensive decision, as it is the one that affects more negatively the other services. This is due to the massive PV curtailment provoked by the use of a very pessimistic forecast ($\text{AnEn}_{\tau=0.1}$). This seems not be worth it, as the improvement on the GC indicator is marginal compared to the performance obtained in this indicator using the other strategies (e.g. 1.2% improvement maximum). Therefore, a good compromise to obtain fairly good performance in all services, seems to be the GPP_{min}-$\text{AnEn}_{\tau=0.4}$ strategy, followed by the EC_{min}-$\text{AnEn}_{\tau=0.5}$ strategy. However, the selection of the strategy that produces the best compromise among all services, will depend on the order of priority among the services dictated by the final user.

The seasonal analyses show that the best accuracy of forecasts and performance of EC, CO2 and GPP is obtained in summer and spring while the worst performance is obtained in winter and autumn. Winter is particularly the season when the price of the electricity is the highest and solar resource is at its lowest, while autumn is the period when the energy is more loaded with CO_2. It is important to remark that there are several variables such as: consumption and PV production profiles, electricity prices and carbon footprint of the grid electricity, that vary throughout the year and in this way, they condition the performance achieved by the EMS strategies. Isolating the effects of each of those variables is out of the scope of this study, however it would be of interest to perform this study in a further stage of the research.

As quantile forecasts allow to customize the scheduling optimization for each season of the year, the implementation of a seasonally-adapted EMS strategy might be plausible. However the results for this study-case, demonstrated that a seasonal EMS strategy is beneficial only regarding the energy-cost, where a decrease of up to 9.1% can be achieved.

Acknowledgments: This work benefited from the support of the Energy4Climate Interdisciplinary Center (E4C) of IP Paris and Ecole des Ponts ParisTech. It was supported by 3rd Programme d'Investissements d'Avenir [ANR-18-EUR-0006-02]

Conflicts of Interest: The authors declare no conflict of interest.The funders had no role in the design of the study; in the collection, analyses, or interpretation of data; in the writing of the manuscript, or in the decision to publish the results.

Appendix A. Nominal and adjusted values for battery and PV energy

Appendix A.1. Energy cost calculations

In this section, the calculations to compute the nominal and adjusted costs of the energy coming from the battery and the PV panels are presented.

The nominal cost for the use of the battery is computed using equation A1.

$$C_{batt}^{nom} = \frac{CAPEX_{batt}}{TOE_{min}} \tag{A1}$$

Preprints (www.preprints.org) | NOT PEER-REVIEWED | Posted: 20 September 2020 doi:10.20944/preprints202009.0461.v1

where $CAPEX_{batt}$ stands for the capital expenditure (the cost) of the battery, while the TOE_{min} stands for the minimum through output energy of the battery or the minimum energy that the manufacturer guarantees that the battery will deliver during its lifetime (see table A1). The TOE_{min} is computed for specific test conditions set by the manufacturer of the battery.

In our case, we assume that TOE_{min} is computed for the nominal battery cycling life CL_{max}. Therefore, when CL decreases, that causes TOE to decrease accordingly, increasing the cost of the energy delivered by the battery in the same proportion. The correction factor for the reduction in the battery cycling life B_{LR}, is presented in equation A2.

The nominal cost of the energy delivered by the battery C^{h}_{batt}, computed in equation A1, is adjusted the equivalent cycling life (CL) of the battery [29], as presented in equation A2.

$$B_{LR} = \frac{CL}{CL_{max}} \tag{A2}$$

where CL is the equivalent battery cycling life while CL_{max} is the maximum (theoretical) battery cycling life according to the model proposed by Muenzen et al. [29].

Then, the factor B_{LR} is used to adjust the nominal cost of the battery presented in equation A1 to obtain the corrected battery cost. This is expressed in equation A3.

$$C^{corr}_{batt} = \frac{C^{nom}_{batt}}{B_{LR}} \tag{A3}$$

Then, for a given EMS strategy, the equivalent B_{LR} can be computed in order to obtain the corrected battery cost C^{corr}_{batt}. This cost is considered constant for the entire test period. For the sake of simplicity, we consider that these average use conditions of the battery are kept throughout all its lifetime, so that the reduction of its cycling life is consistent with the calculations.

An analogous approach as the one presented in equations A1, A2 and A3 can be followed to obtain the average cost of PV energy, C_{pv}.

The nominal cost of the energy delivered by the PV panels C^{nom}_{pv}, can be obtained with the equation A4.

$$C^{nom}_{pv} = \frac{CAPEX_{pv}}{TOE_{exp}} \tag{A4}$$

where $CAPEX_{pv}$ stands for the capital expenditure (the cost) of the PV array (without taking into account the balance-of-system costs), while TOE_{exp} represents the expected through-output-energy, which is computed based on the historical PV output power measurements of the study-case site and the warranted life and output-power of the PV panels given by the manufacturer (see table A1).

In the meantime, an equivalent to the B_{LR} can be found for the PV power production, that is related to the reduction in the through output energy due to curtailment. This is called PV curtailment factor (PV_{CF}) and is expressed in equation A5.

$$PV_{CF} = \frac{E^{potential}_{pv} - E^{curtailed}_{pv}}{E^{potential}_{pv}} = \frac{E^{real}_{pv}}{E^{potential}_{pv}} \tag{A5}$$

where $E^{potential}_{pv}$ is the potential output energy of the PV installation during the test period for the given GHI conditions, while the $E^{curtailed}_{pv}$ represent the total curtailed energy during the test period.

In this case, for a particular EMS strategy, the results of equation A5 are extrapolated as if the curtailment policy were to repeat for the entire life of the PV installation. Under this assumption, equation A3 can be rewritten to compute the corrected cost of the energy delivered by the PV panels, as in equation A6.

$$C^{corr}_{pv} = \frac{C^{nom}_{pv}}{PV_{CF}} \tag{A6}$$

Preprints (www.preprints.org) | NOT PEER-REVIEWED | Posted: 20 September 2020 doi:10.20944/preprints202009.0461.v1

Appendix A.2. Energy CO_2 content calculations

Following a similar method as the one presented in section A.1, in this section the nominal values for the CO_2 content of the energy delivered by the battery and PV, based on their embedded carbon emissions (see table A1) are computed.

The nominal values for the CO_2 content of the battery and PV panels are computed as follow:

$$CO_{2_{batt}}^{nom} = \frac{E_{CO_{2batt}}}{TOE_{min}} \tag{A7}$$

$$CO_{2_{pv}}^{nom} = \frac{E_{CO_{2pv}}}{TOE_{exp}} \tag{A8}$$

where $E_{CO_{2X}}$ stands for the embedded CO_2 emissions expelled to the atmosphere during the manufacturing process of the DER X (see table A1).

The corresponding corrected values for the CO_2 content of battery $CO_{2_{batt}}^{h}$ and PV energy $CO_{2_{pv}}^{h}$, are computed by changing the capital cost $CAPEX_x$ in equations A3 and A6, and replacing it with the embedded CO_2 emissions during manufacturing. In these way, we obtain the relations to compute the corrected values for the CO_2 content of battery and PV energy, as presented in equations A9 and A10.

$$CO_{2_{batt}}^{corr} = \frac{E_{CO_{2batt}}}{TOE_{min} \cdot \frac{CL}{CL_{max}}} = \frac{CO_{2_{batt}}^{nom}}{B_{LR}} \tag{A9}$$

$$CO_{2_{pv}}^{corr} = \frac{E_{CO_{2pv}}}{TOE_{exp} \cdot \frac{E_{pv}^{potential} - E_{pv}^{curtailed}}{E_{pv}^{potential}}} = \frac{CO_{2_{pv}}^{nom}}{PV_{CF}} \tag{A10}$$

The coefficients B_{LR} and PV_{CF} are the same as for the calculations of EC (see equations A2 and A5), as well as the TOE_{min} and TOE_{exp} (see table A1).

A summary of the $CAPEX$ and embedded CO_2 emissions of the battery and PV panels, as well as their nominal energy cost, is presented in table A1. The costs do not include balance-of-system expenses.

In order to compute the through-Output-Energy (TOE), the expected annual PV production is obtained for the study-case site. This calculation is based upon historical GHI measurements during the test period ($\approx$ 1 year). This annual energy output is then extrapolated for the number of years that PV panels are expected to last, according to the manufacturer (30 years with a 0.26% annual degradation). In this way, the -average- total energy that the PV array is expected to deliver throughout its lifetime (TOE) is obtained.

Regarding the TOE value for the battery, it is the minimum -warranted- energy that the battery will deliver during its lifetime, regardless of its profile of use, according to the manufacturer.

The CAPEX costs are based on -average- market prices in Europe for PV panels and Lithium-ion batteries, for the capacity requirements of the Drahi-X MG.

Regarding the embedded CO_2 emissions (greenhouse gases emitted through the manufacturing process, including extraction of raw materials), several studies were consulted and the values were taken from the ones that seemed more adapted to the European case, and to the manufacturing sites of the type of PV panels and batteries expected to be used in the Drahi-X MG. The references used to obtain the TOE, CAPEX and embedded CO_2 emissions (E_{CO_2}) are presented in table A1.

With the aforementioned values, table A1 is completed using equations A7 and A8 to obtain the nominal values of CO_2 content per kWh of energy delivered by the battery and PV panels, respectively. In a similar manner, equations A1 and A4 are used to obtain the nominal cost per kWh delivered by the battery and PV panels, respectively.

Preprints (www.preprints.org) | NOT PEER-REVIEWED | Posted: 20 September 2020 doi:10.20944/preprints202009.0461.v1

Table A1. Nominal cost and CO_2 per kW/h of energy delivered by the battery and PV panels

	TOE(kWh)	**CAPEX**(€)	$\mathbf{E_{CO_2}}(kgCO_2eq)$	$\mathbf{CO_2^{nom}}(gCO_2eq/kWh)$	$\mathbf{C^{nom}}$(€/kWh)
PV (16kWp)	581000 [23]	9265 [30]	19520 [31]	33	0.016
Battery (32kWh)	98100 [32]	20208 [32]	2300 [33]	23	0.210

Appendix B. Optimization algorithms

In this section a description of the optimization algorithms used for the scheduling stage of the EMS as well as the formulation of the objective functions are presented. A genetic algorithm is used to optimize the energy cost (EC) and the CO_2 content (CO2). The flow diagram that describes its working principle is shown in figure A1 and the hyper-parameters obtained after tuning the algorithm are presented in table A2.

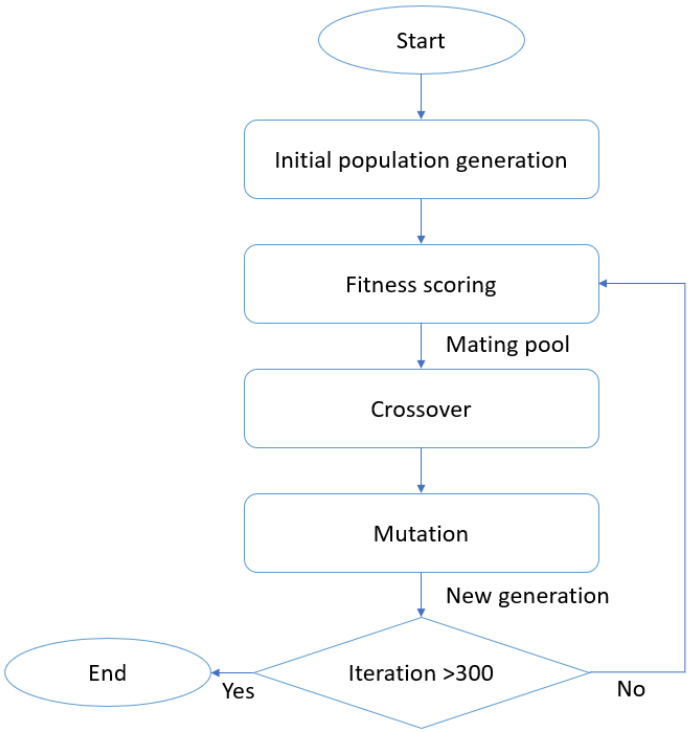

Figure A1. Flow diagram of the genetic algorithm method

Appendix B.1. Energy cost minimization

The energy cost EC, is the first service minimized using the genetic the GA. The costs of the battery and PV energy, included in the objective function (see equation A11), correspond to the constant non-corrected nominal values C^{nom}, presented in table A1. The correction due to battery-life reduction and PV curtailment, expressed in equations A3 and A6, is computed once the grid power profile for the entire test period has been generated. This has to be this way since, as expressed in equations **??** and A5, a prior grid profile is required to compute the correction factors B_{LR} and PV_{CF}. The optimization problem, including the objective function and its constraints, is expressed in the set of equations A11.

$$\underset{P_{batt}}{Min} \sum_{h=1}^{24} \Delta t \cdot (P^h_{grid} \cdot C^h_{grid} + P^h_{batt} \cdot C^h_{batt} + P^h_{pv} \cdot C^h_{pv} + M \cdot P^h_{grid}) + L \cdot SoC_{dev} + K \cdot SoC_{out}$$

Preprints (www.preprints.org) | NOT PEER-REVIEWED | Posted: 20 September 2020 doi:10.20944/preprints202009.0461.v1

Table A2. Summary of the penalization weights and hyper-parameters chosen for the Genetic Algorithm formulation

Penalization weights	
K	$1 \cdot 10^6$
L	5
M	$1 \cdot 10^{-5}$
Hyper-parameters	
# of Iterations	300
Population size	1000
Mutation probability	100%
# of mutating chromosomes	1
Mating pool size (# of parents)	100

where: $\begin{cases} C^h_{batt} = 0 & \text{if } P^h_{batt} < 0 \\ C^h_{grid} = 0 & \text{if } P^h_{grid} < 0 \\ M = 0 & \text{if } P^h_{grid} > 0 \end{cases}$

s.t.

$$P^h_{grid} + P^h_{batt} + P^h_{pv} + P^h_{load} = 0$$

$$\Delta t \cdot \sum_{h=1}^{24} P^h_{batt} = 0 \ (SoC^{h=24} = SoC^{h=1})$$

$$P^h_{pv} = P^{h\ mppt}_{pv}$$

$$0\% \leq SoC^h_{batt} \leq 100\%$$

$$0 \text{ kW} \leq P^h_{batt} \leq 27kW$$

(A11)

where $P^{h\ mppt}_{pv}$ is the maximum possible PV power output of hour h (i.e. the power delivered by the maximum power point tracker -mppt- controller). The energy delivered by the PV panels is the product of its average-hourly power and the time resolution (E^h_{pv}=$P^h_{pv}\Delta t$). The factors M, L and K represent respectively the penalizing weights of: the energy sent to the grid (P^h_{grid}<0), the deviation from the desired SoC at the end of the day (SoC_{dev}) and SoC values that go out-of-bounds (SoC_{out}), for a given battery profile, as previously explained in this section.

It can be observed that the costs of grid and battery energy are zero when these resources consume energy. This is done this way because, in the case of the battery, the TOE_{min} given by the manufacturer refers to delivered energy, while in the case of the grid energy, our study-case SB is not paid if energy is sent back to the grid. The optimization is supposed to be performed once a day (at midnight) when the PV output power forecasts for the next day become available. The SoC of the battery is constrained to be left, by the end of each day, at the same value as it was at the beginning of it, which in this study is set to 50%.

Appendix B.2. CO_2 content minimization

The second service that can be optimized during the scheduling is the CO_2 content of the energy consumed in the MG. This variable is also minimized using the GA approach, as for the EC. Therefore, the CO_2 content of the energy coming from the grid is considered known beforehand for every hour of

Preprints (www.preprints.org) | NOT PEER-REVIEWED | Posted: 20 September 2020 doi:10.20944/preprints202009.0461.v1

the test period (see figure **??**). The formulation of the problem is analogous to the one presented in equation A11. The complete formulation of the problem is presented in equation A12.

$$\underset{P_{batt}}{Min}\ \Delta t \cdot \sum_{h=1}^{24}(P_{grid}^{h} \cdot CO_{2_{grid}}^{h} + P_{batt}^{h} \cdot CO_{2_{batt}}^{h} + P_{pv}^{h} \cdot CO_{2_{pv}}^{h} + M \cdot P_{grid}^{h}) + L \cdot SoC_{dev} + K \cdot SoC_{out}$$

$$\text{where:} \begin{cases} CO_{2_{batt}}^{h} = 0 & \text{if } P_{batt}^{h} < 0 \\ CO_{2_{grid}}^{h} = 0 & \text{if } P_{grid}^{h} < 0 \\ M = 0 & \text{if } P_{grid}^{h} > 0 \end{cases}$$

s.t.

$$P_{grid}^{h} + P_{batt}^{h} + P_{pv}^{h} + P_{load}^{h} = 0$$

$$\Delta t \cdot \sum_{h=1}^{24} P_{batt}^{h} = 0 \ (SoC^{h=24} = SoC^{h=1})$$

$$P_{pv}^{h} = P_{pv}^{h\ mppt}$$

$$0\% \leq SoC_{batt}^{h} \leq 100\%$$

$$0 \text{ kW} \leq P_{batt}^{h} \leq 27kW$$

(A12)

where CO_2 content of the battery and PV energy included in the objective function, correspond to the constant non-corrected nominal values CO_2^{nom}, presented in table A1. The correction due to battery-life reduction and PV curtailment, expressed in equations A9 and A10, is computed once the grid power profile for the entire test period has been generated, for the same reasons exposed for the EC minimization. The factors M, L and K represent respectively the penalizing weights of: the energy sent to the grid (P_{grid}^{h}<0), the deviation from the desired SoC at the end of the day (SoC_{dev}) and SoC values that go out-of-bounds (SoC_{out}), for a given battery profile, as previously explained in this section.

Appendix B.3. Grid peak-power minimization

The third service that was envisaged to be optimized by the scheduling module was the required contracted power or grid-peak-power (GPP). Due to the nature of its objective function, a typical quadratic programming formulation sufficed to solve the optimization problem. The simple formulation, convergence speed, as well as its ability to find true optimal solutions, made us prefer this method over the GA to optimize this service. The minimization of the GPP hereby proposed, falls into the category of quadratic programming problems. Quadratic programming is the process of solving a linearly constrained, quadratic optimization problem, that is, the problem of optimizing (minimizing or maximizing) a quadratic function of several variables subject to linear constraints on these variables. Quadratic programming is a particular type of non-linear programming (NLP) [34]. The formulation of the optimization problem is presented in equation A13. We observe that the same physical constraints as for the GA formulation are present in this problem (see equations A11 and A12).

$$\underset{P_{grid}, P_{batt}}{Minimize}\ \sum_{h=1}^{24}({P_{grid}^{h}}^{2} + {P_{batt}^{h}}^{2})$$

s.t.

$$
\begin{aligned}
\mathrm{P}^{h}_{grid} + P^{h}_{batt} + P^{h}_{pv} + P^{h}_{load} &= 0 \\
\Delta t \cdot \textstyle\sum_{h=1}^{24} P^{h}_{batt} &= 0 \ (SoC^{h=24} = SoC^{h=1}) \\
\mathrm{P}^{h}_{pv} &= P^{h\ mppt}_{pv} \\
0\% \leq SoC^{h}_{batt} &\leq 100\% \\
0 \ \mathrm{kW} \leq P^{h}_{grid} &\leq 36kW \\
0 \ \mathrm{kW} \leq P^{h}_{batt} &\leq 27kW
\end{aligned}
$$

(A13)

We can note that here there are no costs associated to the power values, as the algorithm is only meant to minimize the peaks of power themselves, trying to make the profile as smooth as possible.

As deduced from its objective function, the method minimizes the power peaks of the grid and the battery simultaneously, reducing not only the required contracted power, but also the depth-of-discharge of the battery, which might lead to extended battery life. There is no associated costs to the grid or battery power, as the power profile itself suffices for the optimizer to obtain the required results. As for the EC and CO2, once the algorithm generates the resulting grid and battery profiles for the entire test period, all the performance indicators can be computed and the grid profile is used as the input for the balancing module.

Contrary to heuristic methods such as the GA, quadratic programming methods do not required the tuning of hyper-parameters, which diminish the setting-up time and the uncertainty of obtaining sub-optimal solutions.

1. Zia, M.F.; Elbouchikhi, E.; Benbouzid, M. Microgrids energy management systems: A critical review on methods, solutions, and prospects. *Applied Energy* **2018**, *222*, 1033–1055. doi:10.1016/j.apenergy.2018.04.103.
2. Minchala-Avila, L.I.; Garza-Castañón, L.E.; Vargas-Martínez, A.; Zhang, Y. A Review of Optimal Control Techniques Applied to the Energy Management and Control of Microgrids. *Procedia Computer Science* **2015**, *52*, 780–787. doi:10.1016/j.procs.2015.05.133.
3. Herath, A.; Kodituwakku, S.; Dasanayake, D.; Binduhewa, P.; Ekanayake, J.; Samarakoon, K. Comparison of Optimization- and Rule-Based EMS for Domestic PV-Battery Installation with Time-Varying Local SoC Limits. *Journal of Electrical and Computer Engineering* **2019**, *2019*, 1–14. doi:10.1155/2019/8162475.
4. Ahmad Khan, A.; Naeem, M.; Iqbal, M.; Qaisar, S.; Anpalagan, A. A compendium of optimization objectives, constraints, tools and algorithms for energy management in microgrids. *Renewable and Sustainable Energy Reviews* **2016**, *58*, 1664–1683. doi:10.1016/j.rser.2015.12.259.
5. Khodaei, A.; Bahramirad, S.; Shahidehpour, M. Microgrid Planning Under Uncertainty. *IEEE Transactions on Power Systems* **2015**, *30*, 2417–2425. doi:10.1109/TPWRS.2014.2361094.
6. Li, Z.; Zang, C.; Zeng, P.; Yu, H. Combined Two-Stage Stochastic Programming and Receding Horizon Control Strategy for Microgrid Energy Management Considering Uncertainty. *Energies* **2016**, *9*, 499. doi:10.3390/en9070499.
7. Mazzola, S.; Vergara, C.; Astolfi, M.; Li, V.; Perez-Arriaga, I.; Macchi, E. Assessing the value of forecast-based dispatch in the operation of off-grid rural microgrids. *Renewable Energy* **2017**, *108*, 116–125. doi:10.1016/j.renene.2017.02.040.
8. Sachs, J.; Sawodny, O. A Two-Stage Model Predictive Control Strategy for Economic Diesel-PV-Battery Island Microgrid Operation in Rural Areas. *IEEE Transactions on Sustainable Energy* **2016**, *7*, 903–913.
9. Parisio, A.; Wiezorek, C.; Kyntaja, T.; Elo, J.; Johansson, K.H. An MPC-based Energy Management System for multiple residential microgrids. 2015 IEEE International Conference on Automation Science and Engineering (CASE), 2015, pp. 7–14.

10. Liu, G.; Xu, Y.; Tomsovic, K. Bidding Strategy for Microgrid in Day-Ahead Market Based on Hybrid Stochastic Robust Optimization. *IEEE Transactions on Smart Grid* **2016**, *7*, 227–237.
11. Bogaraj, T.; Kanakaraj, J. Intelligent energy management control for independent microgrid. *Sādhanā* **2016**, *41*, 755–769. doi:10.1007/s12046-016-0515-6.
12. Olivares, D.E.; Lara, J.D.; Canizares, C.A.; Kazerani, M. Stochastic-Predictive Energy Management System for Isolated Microgrids. *IEEE Transactions on Smart Grid* **2015**, *6*, 2681–2693.
13. Dou, C.X.; An, X.G.; Yue, D. Multi-agent System Based Energy Management Strategies for Microgrid by using Renewable Energy Source and Load Forecasting. *Electric Power Components and Systems* **2016**, *44*, 2059–2072. Publisher: Taylor & Francis _eprint: https://doi.org/10.1080/15325008.2016.1210699, doi:10.1080/15325008.2016.1210699.
14. Adinolfi, F.; D'Agostino, F.; Massucco, S.; Saviozzi, M.; Silvestro, F. Advanced operational functionalities for a low voltage Microgrid test site. 2015 IEEE Power Energy Society General Meeting, 2015, pp. 1–5.
15. Agüera-Pérez, A.; Palomares-Salas, J.C.; González de la Rosa, J.J.; Florencias-Oliveros, O. Weather forecasts for microgrid energy management: Review, discussion and recommendations. *Applied Energy* **2018**, *228*, 265–278. doi:10.1016/j.apenergy.2018.06.087.
16. Global Renewables Outlook: Energy Transformation 2050. website, 2020. [retrieved:3-4-2020], https://www.irena.org/publications/2020/Apr/Global-Renewables-Outlook-2020.
17. Tao, L.; Mancarella, P.; Hatziargyriou, N.; Buchhoz, B.; Schwaegerl, C.; Strbac, G. European Roadmap for Microgrids. website, 2010. [retrieved:5-4-2020], url = https://www.joinup.ec.europa.eu.
18. Hatziargyriou, N.D.; Anastasiadis, A.G.; Tsikalakis, A.G.; Vasiljevska, J. Quantification of economic, environmental and operational benefits due to significant penetration of Microgrids in a typical LV and MV Greek network. *European Transactions on Electrical Power* **2011**, *21*, 1217–1237. _eprint: https://onlinelibrary.wiley.com/doi/pdf/10.1002/etep.392, doi:10.1002/etep.392.
19. Strbac, G.; Hatziargyriou, N.; Lopes, J.P.; Moreira, C.; Dimeas, A.; Papadaskalopoulos, D. Microgrids: Enhancing the Resilience of the European Megagrid. *IEEE Power and Energy Magazine* **2015**, *13*, 35–43. doi:10.1109/MPE.2015.2397336.
20. Calderon-Obaldia, F.; Le Gal La Salle, J.; Badosa, J.; Lauret, P.; Migan-Dubois, A.; Bourdin, V. Uncertainty estimation for deterministic solar irradiance forecasts based on analogs ensembles.
21. Alessandrini, S.; Delle Monache, L.; Sperati, S.; Cervone, G. An analog ensemble for short-term probabilistic solar power forecast. *Applied Energy* **2015**, *157*, 95–110. doi:10.1016/j.apenergy.2015.08.011.
22. Badosa, J.; Gobet, E.; Grangereau, M.; Kim, D. Day-Ahead Probabilistic Forecast of Solar Irradiance: A Stochastic. *Renewable Energy: Forecasting and Risk Management: Paris, France, June 7-9, 2017* **2018**, *254*, 73.
23. Haeffelin, M.e.a. SIRTA, a ground-based atmospheric observatory for cloud and aerosol research. *Annales Geophysicae* **2005**, *23*, 253–275.
24. Tarif Tempo EDF : Grille tarifaire en 2020 et CGV, 2018. Library Catalog: prix-elec.com.
25. Eco2mix CO2, 2014. Library Catalog: www.rte-france.com.
26. Ferruzzi, G.; Cervone, G.; Delle Monache, L.; Graditi, G.; Jacobone, F. Optimal bidding in a Day-Ahead energy market for Micro Grid under uncertainty in renewable energy production. *Energy* **2016**, *106*, 194–202. doi:10.1016/j.energy.2016.02.166.
27. Chaouachi, A.; Kamel, R.M.; Andoulsi, R.; Nagasaka, K. Multiobjective Intelligent Energy Management for a Microgrid. *IEEE Transactions on Industrial Electronics* **2013**, *60*, 1688–1699. doi:10.1109/TIE.2012.2188873.
28. Mohamed, F.A.; Koivo, H.N. Multiobjective optimization using Mesh Adaptive Direct Search for power dispatch problem of microgrid. *International Journal of Electrical Power & Energy Systems* **2012**, *42*, 728–735. doi:10.1016/j.ijepes.2011.09.006.
29. Muenzel, V.; de Hoog, J.; Brazil, M.; Vishwanath, A.; Kalyanaraman, S. A Multi-Factor Battery Cycle Life Prediction Methodology for Optimal Battery Management. Proceedings of the 2015 ACM Sixth International Conference on Future Energy Systems; Association for Computing Machinery: Bangalore, India, 2015; e-Energy '15, pp. 57–66. doi:10.1145/2768510.2768532.
30. Solar photovoltaic panels distribuitor. website, 2020. [retrieved:3-4-2020], https://www.europe-solarstore.com/.
31. Yue, D.; You, F.; Darling, S.B. Domestic and overseas manufacturing scenarios of silicon-based photovoltaics: Life cycle energy and environmental comparative analysis. *Solar Energy* **2014**, *105*, 669–678. doi:10.1016/j.solener.2014.04.008.

32. BYD Li-Ion batteries distribuitor. website, 2020. [retrieved:3-4-2020], https://www.mg-solar-shop.com/byd-b-box-l-10.5-battery-storage-10.5-kwh.
33. Majeau-Bettez, G.; Hawkins, T.R.; Strømman, A.H. Life Cycle Environmental Assessment of Lithium-Ion and Nickel Metal Hydride Batteries for Plug-In Hybrid and Battery Electric Vehicles. *Environmental Science & Technology* **2011**, *45*, 4548–4554. doi:10.1021/es103607c.
34. Nocedal, J.; Wright, S.J. *Numerical optimization*; New York : Springer, 2006.

 doi:10.20944/preprints202009.0461.v1

Sample Availability: Samples of the compounds ..... are available from the authors.